A Method for Higher Accuracy Ampacity Calculation of Rectangular, Universal Angle, and Integral Web Substation Bus

Joseph Goldenburg, *Member, IEEE*, and Anthony Pribble, *Member, IEEE*

***Abstract*—Substation bus ampacity calculations perform a steady-state heat transfer analysis on a unit length of bus. In this analysis, the convective heat transfer coefficients for rectangular, universal angle bus (UAB), and integral web bus conductor (IWBC) have historically been calculated by applying flat plane correlations to the individual bus surfaces. The research presented here will show that the Nusselt correlations developed for the specific bus, similar to what is currently used for round bus, increases accuracy in bus ampacity predictions. Additionally, the correlations are easier to use and less likely to result in calculation error. This paper presents natural and forced convection correlations for rectangular, universal angle bus, and integral web bus.**

***Index Terms*—Ampacity, bus, cooling, heat-transfer, substation, Temperature, Nusselt-number, rayleigh-number, forced-convection, natural-convection.**

I. Introduction

SUBSTATION bus ampacity ratings are commonly calculated by performing an energy balance on a unit length of bus [1]. Ampacity limits are set to control bus temperature, prevent strength loss from excessive heating, or damage to attached equipment from thermal conduction. Solving the energy balance equation accurately helps prevent undesirable effects.

The present substation bus ampacity calculation method used in IEEE standard 605 appeared in 1976 with the publication by Prager, Pemberton, Craig, and Bleshman [2]. Their method involves decomposing bus geometries into a series of flat planes and calculating the convective heat transfer coefficient from each plane. The calculated coefficients are summed to find the total convective heat loss. The method is applicable to common substation bus geometries such as rectangular, universal angle, and integral web. This method was adopted by IEEE standard 605 and is still employed today. While the work created an analytical method for calculating bus ampacity, no experimental data could be located to support its use.

Manuscript received June 26, 2019; revised September 9, 2019; accepted October 12, 2019. Date of publication October 18, 2019; date of current version July 23, 2020. This work was supported by the members of the National Electric Energy Testing Research and Application Center. Paper no. TPWRD-00695-2019. *(Corresponding author: Joseph Goldenburg.)*

The authors are with the National Electric Energy Testing Research and Application Center, Forest Park, GA 30297 USA (e-mail: joe.goldenburg@neetrac.gatech.edu; tony.pribble@neetrac.gatech.edu).

Color versions of one or more of the figures in this article are available online at http://ieeexplore.ieee.org.

Digital Object Identifier 10.1109/TPWRD.2019.2948271

Tubular bus, which is not composed of flat planes, uses a Nusselt correlation developed specifically for round geometries. A literature search was conducted and one publication was found that verifies the model for tubular bus [3]. The search showed much of the present bus ampacity work focuses on predicting temperatures of busduct systems through Finite Element or numerical analysis methods [4]–[6], leaving a gap in the research. As North American utilities are required to justify their ampacity calculation method as ordered in NERC Standard FAC-008-3, providing experimental data for rectangular, universal angle and integral web bus will support their efforts for reliable power delivery.

This work determined the accuracy of the convective portion of the Prager, Pemberton, Craig, and Bleshman model through laboratory wind tunnel experiments and computational fluid dynamic simulations.

Further, an alternative method to calculate the convective heat transfer coefficient is presented.

Nusselt correlations for 3-Dimensional shapes such as triangular, square, hexagonal, octagon, oval, spherical, and toroidal exist [8]–[10]. Several of these shapes are candidates for the flat plane correlation method described previously. While the flat plane method inherently assumes flow is laminar over all surfaces and is at a constant velocity, numerous experiments have shown that the average convective heat transfer coefficient relates to the true flow regime (e.g., laminar, turbulent, or mixed) [11]. In contrast, a specifically developed Nusselt correlation relates the actual flow conditions to the average convective heat transfer coefficient since the correlation uses the Reynolds number to characterize the current flow state around the object. A literature search was conducted in an attempt to locate Nusselt correlations for commonly used substation bus geometries. One resource contained correlations for vertically oriented rectangles in crosswise airflow [9]. No other correlations or geometries were located.

Nusselt correlations for rectangular, universal angle, and integral web bus were developed from the collected data. The accuracy was found and compared to the method from Prager, Pemberton, Craig, and Bleshman.

II. Heat Transfer Methodology

For both forced and natural convection, the steady state equation for heat transfer from a unit length of substation bus at

0885-8977 © 2019 IEEE. Personal use is permitted, but republication/redistribution requires IEEE permission.
See https://www.ieee.org/publications/rights/index.html for more information.

Authorized licensed use limited to: Georgia Institute of Technology. Downloaded on September 09,2020 at 14:47:32 UTC from IEEE Xplore. Restrictions apply.

constant temperature is:

$$\mathrm{I^2R + Q_{solar} = Q_{convection} + Q_{radiation}} \quad (1)$$

A. Forced Convection

Forced convection heat transfer is calculated through:

$$\mathrm{Q_{convection} = hA\Delta T} \quad (2)$$

Where:

h	is the heat transfer coefficient, $[\mathrm{W/m^2\ ^\circ C}]$
A	is the surface area of the bus, $[\mathrm{m^2}]$
ΔT	is the temperature difference between the bus and environment, $[^\circ\mathrm{C}]$

For a given geometry, the forced convection heat transfer coefficient *h* is correlated with air velocity through the relationship [11]:

$$\mathrm{Nu} = \frac{\mathrm{hL}}{\mathrm{k}} = \mathrm{C(Re^m)Pr^{0.3}} \quad (3)$$

Where:

Nu	is the Nusselt number
h	is the average heat transfer coefficient, $[\mathrm{W/m^2\ ^\circ C}]$
L	is the characteristic length for a specific geometry, [m]
k	is the thermal conductivity of the fluid, $[\mathrm{W/m^\circ C}]$
Re	is the Reynolds number
Pr	is the Prandtl number, typically taken as 0.7 for air.
C and *m*	are empirical constants specific to a geometric shape and orientation.

Note also that:

$$\mathrm{Re} = \frac{\mathrm{VL}}{\nu} \quad (4)$$

Where:

Re	is the Reynolds number
V	is the velocity of the fluid [m/s]
L	is the characteristic length for a specific geometry, [m]
υ	is the kinematic viscosity of the fluid, $[\mathrm{m^2/s}]$

Research performed by numerous authors have shown that Nusselt correlations for forced flow conditions follow the general form in (3) [8]–[11]. The work of Prager, Pemberton, Craig, and Bleshman makes use of the correlation developed by other researchers [11] for a horizontal plane, where *C* in (3) equals 0.664 and *m* equals ½. It is applied to each surface of the bus independently and regardless of orientation. The convective heat transfer coefficients calculated for a vertical surface therefore are the same as that of a horizontal surface of equivalent length. This implies the flow field around a bus does not depend on orientation, which is likely incorrect. This also means the method does not characterize forced convective heat transfer for a complex bus geometry, such as integral web, with a set of specific *C* and *m* values.

In this work, new Nusselt correlations are developed from experimental and simulation data for typical substation bus geometries and orientations. In other words, the constants *C* and *m* in (3) are determined by experiment, enabling a calculation for *h* from a single equation.

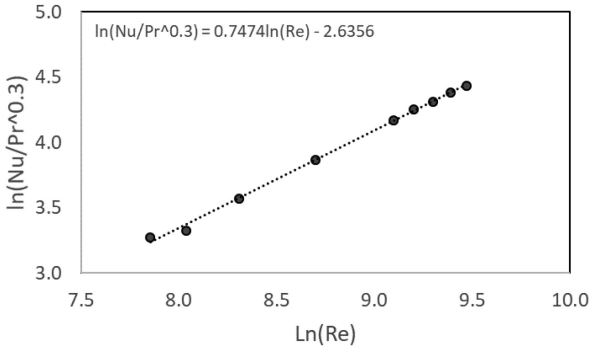

Fig. 1. Log-log plot of experimental data.

To achieve this, a bus sample is heated until it reaches a steady state temperature where the energy balance in (1) applies. The recorded data is used to calculate *Nu*, *Re*, and *Pr*. After several trials varying fluid velocity, temperatures, and geometry size, a plot of $\ln(\mathrm{Nu/Pr^{0.3}})$ vs. ln(Re) is created. Fig. 1 is an example of such a plot. A linear trend line is fit to the data. The coefficient *m* is the slope of the trend line and *C* is found by taking the exponential of the intercept term. Once found, (3) is used to calculate the convective heat transfer coefficient, *h*. Notice *C* and *m* are valid over a specific Reynolds range as points outside the range may have different constants. Flow transition, such as laminar to turbulent, will cause the coefficients to change and affect the Nusselt correlation. This was accounted for in the experimental design.

Standard bus sizes were taken from a common substation bus manufacturer's catalog. The smallest standard bus size for each geometry with an assumed 0.6 m/s (2 ft/s) air velocity was used to calculate a lower target Reynolds number. The upper target took the largest standard bus size and an assumed 2 m/s (6.6 ft/s) air velocity. The Nusselt correlations developed and presented in Section IV are therefore valid for all standard bus sizes at the industry standard assumption of 0.6 m/s (2 ft/s) air velocity.

B. Natural Convection

Heat transfer via natural convection is calculated the same as in (2). For a given geometry, the natural convection heat transfer coefficient *h* can be found by correlating the Nusselt number with the Rayleigh number through the relationship:

$$\mathrm{Nu} = \frac{\mathrm{hL}}{\mathrm{k}} = \mathrm{C(Ra^m)} \quad (5)$$

Where:

Nu	is the Nusselt number
h	is the average heat transfer coefficient, $[\mathrm{W/m^2\ ^\circ C}]$
L	is the characteristic length for a specific geometry, [m]
k	is the thermal conductivity of the fluid, $[\mathrm{W/m^\circ C}]$
Ra	is the Rayleigh number
C and *m*	are empirical constants specific to a geometric shape and orientation.

Authorized licensed use limited to: Georgia Institute of Technology. Downloaded on September 09,2020 at 14:47:32 UTC from IEEE Xplore. Restrictions apply.

Fig. 2. Wind tunnel for forced convection experiments.

Note also that:

$$\mathrm{Ra} = \frac{\mathrm{C_p}\rho^2 \mathrm{g}\beta\Delta\mathrm{TL}^3}{\mu \mathrm{k}} \tag{6}$$

Where:

Ra	is the Rayleigh number
C_p	is the specific heat capacity of the fluid at constant pressure, [J/kg °C]
L	is the characteristic length for a specific geometry, [m]
μ	is the dynamic viscosity of the fluid, [kg/ms]
g	is the gravitational constant, [m/s^2]
ρ	is the density of the fluid, [kg/m^3]
k	is the thermal conductivity of fluid, [W/m°C]
β	is the volumetric thermal expansion coefficient of the fluid, taken as the reciprocal of the film temperature for ideal gases, [1/°C]

The natural convection portion of Prager, Pemberton, Craig, and Bleshman is similar to that of forced convection, except two flat plane correlations are employed; one for vertical and upward facing surfaces, the other for downward facing surfaces. This change results in ampacities that are orientation discriminant. However, this does not capture the true dynamic effects of airflow around a real body.

As is the case for forced convection, new natural convection Nusselt correlations were developed for typical substation bus geometries and orientations. Plots of ln(Nu) vs. ln(Ra) from experimental and simulated data are used to find the constants *C* and *m* of (5). The correlations are accurate over the specified Rayleigh range as the largest and smallest standard bus sizes were again used to create target ranges.

III. Experiments and Simulation Methodology

A. Forced Convection Experiments and Simulations

A wind tunnel was constructed to create controlled, uniform laminar air velocity, as shown in Fig. 2. Air velocity was measured and checked for uniformity at the beginning and end of each test by a hand-held hot wire anemometer. It was inserted approximately 1-foot in front of the leading edge of the bus into the sample chamber. Three (3) air velocity measurements were taken at points corresponding to 0.25, 0.5, and 0.75 of the sample bus length.

Wind tunnel experiments were performed on five different bus shapes and orientations: Horizontal rectangular, vertical rectangular, UAB open, UAB closed, and IWBC. The buses were painted to create a surface of known emissivity ($\varepsilon = 0.95$) as measured at room temperature by Surface Optic's ET100 emissometer. Nine thermocouples were inserted along the full bus length that monitored temperature to ensure no thermal gradients existed across a 2-feet sample length. A known DC current was then applied to the bus and held until a steady state temperature was achieved. The voltage drop across the sample length was measured and the heat generated in the length found using the equation:

$$\mathrm{Q_{heat\ generated}} = \mathrm{VI} \tag{7}$$

Where:

$Q_{heat\ generation}$	is the heat generated in the bus, [J/m^3]
V	is the voltage drop across the length, [V]
I	is the current through the length, [A]

The tunnel air velocity and applied current were varied to create a data set over the target Reynolds range. Equation (1) was then solved and the Nusselt and Reynolds numbers calculated. The *C* and *m* coefficients were found from the data.

Computational Fluid Dynamic (CFD) simulations were also run to confirm the results collected in forced convection experiments. A 2D cross section of the sample and surroundings was constructed in ANSYS Fluent R15.0 Academic for steady state simulations. The ambient temperature, surface emissivities, surface temperatures, air velocity, local atmospheric pressure, and heat generation density were input. The solver ran until it converged on a solution. The heat lost via convection and radiation was recorded and compared to expected values from solving (1) with experimental data. The simulated bus temperatures fell within approximately ±5 °C of the measured bus temperatures, validating the experimental data. A total of 103 experiments and 64 simulations were performed. Table I compares the results of selected experiments and simulations. Fig. 3 is a static temperature plot of universal angle bus in the closed configuration. Fig. 5 provides the geometries tested.

B. Natural Convection Experiments and Simulations

Buses of each geometry and orientation were placed in a draft-free enclosure, as shown in Fig. 4. A hot-wire anemometer was used to verify still-air conditions existed within the enclosure at the start of the test. The buses were painted to create a surface of known emissivity. Nine thermocouples were inserted along its full length and bus temperature was monitored to ensure that no thermal gradients existed across the sample length. A known DC current was then applied to the bus and held until a steady state temperature was achieved. The voltage drop across a unit length of bus was measured and the heat generated found using (7).

Authorized licensed use limited to: Georgia Institute of Technology. Downloaded on September 09,2020 at 14:47:32 UTC from IEEE Xplore. Restrictions apply.

TABLE I
SELECTED FORCED CONVECTION EXPERIMENTS AND SIMULATION COMPARISON

Geometry	Power Density (W/m^3)	Experimental Bus Temperature (°C)	Simulation Bus Temperature (°C)
Horizontal Rectangular	485,089[a]	110.1	105.5
	620,165[b]	115.7	116
	592,562[c]	90.2	91.7
Vertical Rectangular	489,199[a]	90.6	95.1
	943,425[b]	120.6	119.9
	846,857[c]	88.5	94
UAB Closed	950,925[a]	122.8	120.2
	1,216,121[b]	120.8	121.2
	1,754,335[c]	121.8	119.7
UAB Open	561,019[a]	90.1	87.8
	1,076,090[b]	120.2	118
	1,049,998[c]	90.9	90.2
IWBC	586,348[a]	93.0	88.9
	707,416[b]	90.7	89
	1,050,410[c]	91.2	95.9

Air Velocity: [a]0.6 m/s, [b]1 m/s, [c]2 m/s

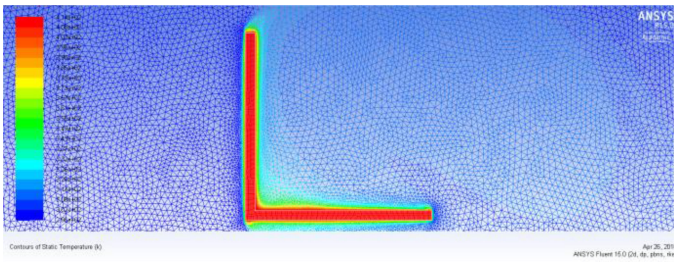

Fig. 3. Static temperature plot of UAB closed in forced convection.

In forced convection, the required range was achieved by primarily varying air velocity within the experimental set up. However, in natural convection experiments, the required Rayleigh ranges cannot be achieved experimentally by changing temperature alone. Instead, multiple bus sizes are needed. As the DC power supply used did not have the required power capacity to heat the largest substation bus sizes available, simulations were used to generate data for larger buses.

Buses of one size were subjected to three experimental trials. Different currents were applied to change the steady state temperature and the data was used to validate a CFD simulation model. The bus sizes were then varied in the CFD simulations to achieve the required Rayleigh range. Once the correlation was developed, a steel or aluminum bus of a different size was constructed for physical experiments, and results used to validate the correlation created from the simulation data. A total of 30 experiments and 69 simulations were performed.

Fig. 4. Draft free enclosure for natural convection experiments.

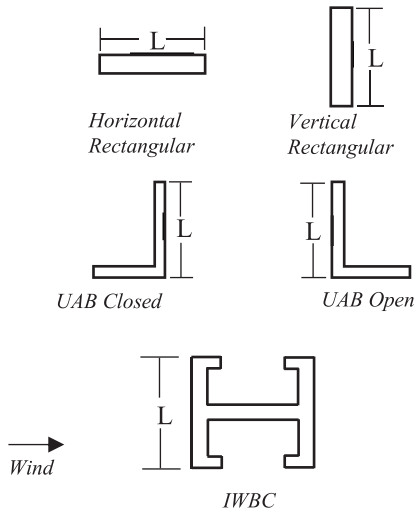

Fig. 5. Bus geometries and orientations for forced convection correlations.

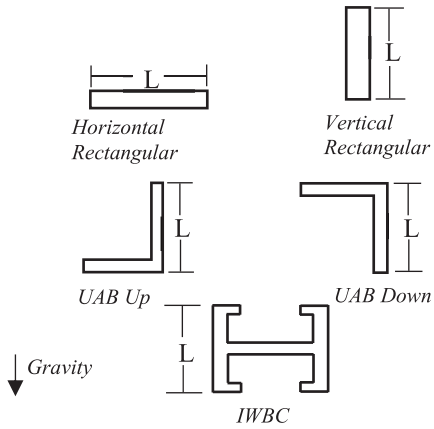

Fig. 6. Bus geometries and orientations for natural convection correlations.

IV. RESULTS

The following geometries and orientations shown in Figs. 5 and 6 were investigated. For each case in Fig. 5, incident wind approaches from the left hand side. In Fig. 6, gravity acts in the downward direction. The characteristic length used to fit the correlation is defined for each geometry as *L*. Note that

Authorized licensed use limited to: Georgia Institute of Technology. Downloaded on September 09,2020 at 14:47:32 UTC from IEEE Xplore. Restrictions apply.

TABLE II
SELECTED NATURAL CONVECTION EXPERIMENTS AND SIMULATION COMPARISON

Geometry	Power Density (W/m^3)	Experimental Bus Temperature (°C)	Simulation Bus Temperature (°C)
Horizontal Rectangular	184,268	69.9	70.6
	335,961	98.9	99.9
	559,025	133.2	133.8
Vertical Rectangular	224,571	69.1	71.3
	439,138	101.0	104.2
	659,999	128.8	133.5
UAB Up	386,274	74.5	74.7
	689,906	103.1	103.0
	990,841	129.5	129.4
UAB Down	347,132	70.2	69.2
	661,685	102.7	99.8
	994,935	130.5	128.3
IWBC	308,806	70.1	70.6
	559,281	99.3	100.2
	892,433	131.5	132.6

TABLE III
FORCED CONVECTION CORRELATION CONSTANTS

Geometry	C	m	Reynold's Range
Horizontal Rectangular	0.21	0.64	250 – 19,000
Vertical Rectangular	0.30	0.63	500 – 22,000
UAB Closed	0.072	0.75	2,500 – 13,000
UAB Open	0.085	0.70	2,800 – 13,000
IWBC	0.038	0.76	2,900 – 27,500

TABLE IV
NATURAL CONVECTION CORRELATION CONSTANTS

Geometry	C	m	Rayleigh's Range
Horizontal Rectangular	0.47	0.20	$2.4x10^4 – 8.5x10^8$
Vertical Rectangular	0.28	0.26	$2.4x10^4 – 8.5x10^8$
UAB Up	0.26	0.25	$7.1x10^6 – 5.9x10^7$
UAB Down	0.17	0.27	$7.1x10^6 – 6.3x10^7$
IWBC	0.20	0.23	$1.5x10^6 – 8.4x10^8$

for UAB, forced and natural convection have different orientations. Table II compares the results of selected experiments and simulations.

A. Forced Convection Correlations

Table III provides the forced convection correlation constants for use in (3) as well as the associated Reynolds range.

B. Natural Convection Correlations

Table IV provides the natural convection correlation constants for use in (5).

V. DISCUSSION

A. Existing Methodology Accuracy for Convection Calculations of Flat Planes

Ambient temperature, air velocity, and bus temperature measured during experiments were used to calculate ampacity with the method described in [1]. This was compared to the current applied during the experiment. Results from forced convection are shown in Table V and natural convection results are shown in Table VI.

The flat plane correlation method over-predicted ampacity in 12 of the 15 forced convection trials studied. Rectangular bus oriented horizontally had an average, over-predicted error of 9.2%. Re-orienting the same bus into a vertical position resulted in under-predicted ampacity with average error of 5.67%. The flat plane method over-predicted ampacity in all universal angle bus trials. Similar to rectangular, reorienting the bus from an open position to a closed position reduced error by 6.84%. Orientation has a significant impact on the method's accuracy. As of now, IEEE 605 and utility engineers use the same ampacity rating regardless of orientation yet, as shown, orientation is not a negligible effect.

Further, the flat plane correlation method over-predicted the ampacity of integral web bus with an average error of 22.3%. The higher error comes from, one, having more surfaces than any other geometry evaluated and, two, by treating all interior surfaces as downward facing surfaces exposed to natural convection.

Results from natural convection experiments show that, once again, flat plane correlations over-predict ampacity. However, the error is less and differences between orientations are reduced. The factors contributing to this are likely to be the method already taking surface orientation into account, and the relation of bus size to Rayleigh number.

Forced convection relates the Reynolds number in (4) to the Nusselt number while natural convection uses the Rayleigh number shown in (6). The Reynolds number scales to the first power with both bus size, as captured in the characteristic length, and air velocity. By comparison, the Rayleigh number scales with a ratio of air properties and the cube of characteristic length. At the temperature ranges substation bus normally operate in, air properties do not change significantly. Therefore, appreciable changes in the Rayleigh number come primarily from changes in bus size. Unlike forced convection, in which air velocity was controlled while bus size was held constant, natural convection experiments changed bus temperature and had the same bus size as a result of power supply limitations. It is possible the flat plane method accuracy varies with bus size beyond the error shown in this work.

B. Proposed Methodology Accuracy for Convection Calculations

In forced convection, the Nusselt correlations developed were least accurate with IWBC (Average error = 5.2%) and most accurate with vertical rectangular (Average error = 1.10%). Except for IWBC, all other geometries and orientations had an

Authorized licensed use limited to: Georgia Institute of Technology. Downloaded on September 09,2020 at 14:47:32 UTC from IEEE Xplore. Restrictions apply.

TABLE V
FORCED CONVECTION FLAT PLANE CORRELATION COMPARED TO PROPOSED NUSSELT CORRELATION

Geometry	Case	Experimental Current Measurement (A)	Existing Ampacity Calculation for Flat Planes (Abs. % error)	Proposed Ampacity Calculation Method (Abs. % error)	Error Reduction[1]
Horizontal Rectangular	1	1295	1425 (10.0)	1338 (3.30)	67.0%
	2	1456	1604 (10.2)	1523 (4.60)	54.9%
	3	1452	1560 (7.40)	1530 (5.40)	27.0%
Vertical Rectangular	1	1323	1286 (2.80)	1314 (0.68)	75.7%
	2	1784	1716 (3.80)	1782 (0.11)	97.1%
	3	1741	1560 (10.4)	1697 (2.50)	76.0%
UAB Closed					
	1	1459	1631 (11.8)	1436 (1.60)	86.4%
	2	2488	2646 (6.40)	2424 (2.60)	59.4%
	3	2944	3065 (4.10)	2979 (1.20)	70.7%
UAB Open					
	1	1153	1351 (17.2)	1123 (2.60)	84.9%
	2	1558	1808 (16.0)	1530 (1.80)	88.8%
	3	1576	1727 (9.60)	1501 (4.80)	50.0%
IWBC					
	1	1001	1320 (31.9)	965 (3.60)	88.7%
	2	1367	1671 (22.2)	1282 (6.20)	72.1%
	3	1341	1514 (12.9)	1263 (5.80)	55.0%

1 Error Reduction = (Existing Ampacity Calculation Error – Proposed Ampacity Calculation Error)/(Existing Ampacity Calculation Error)

TABLE VI
NATURAL CONVECTION FLAT PLANE CORRELATION COMPARED TO PROPOSED NUSSELT CORRELATION

Geometry	Case	Experimental Current Measurement (A)	Existing Ampacity Calculation for Flat Planes (Abs. % error)	Proposed Ampacity Calculation Method (Abs. % error)	Error Reduction[1]
Horizontal Rectangular	1	843	881 (4.5)	827 (1.9)	57.8%
	2	1110	1167 (5.2)	1082 (2.5)	51.9%
	3	1389	1451 (4.4)	1337 (3.8)	13.6%
Vertical Rectangular	1	928	1001 (7.9)	914 (1.5)	81.0%
	2	1258	1344 (6.8)	1206 (4.1)	39.7%
	3	1505	1598 (6.2)	1422 (5.5)	11.3%
UAB Up					
	1	1156	1228 (6.2)	1163 (1.8)	71.0%
	2	1509	1576 (4.4)	1471 (1.4)	68.2%
	3	1775	1842 (3.8)	1708 (2.8)	26.3%
UAB Down					
	1	971	1033 (6.4)	997 (2.7)	57.8%
	2	1253	1339 (6.9)	1272 (1.5)	78.3%
	3	1517	1588 (4.7)	1493 (1.6)	66.0%
IWBC					
	1	2209	2568 (16.3)	2041 (7.6)	53.4%
	2	2856	3311 (16.0)	2599 (9.0)	43.8%
	3	2989	3473 (16.2)	2722 (8.9)	45.1%

1 Error Reduction = (Existing Ampacity Calculation Error – Proposed Ampacity Calculation Error)/(Existing Ampacity Calculation Error)

average error of less than 5%. In these instances, orientation does not affect accuracy as each correlation was developed for a specific geometry and orientation.

Data from natural convection experiments show similar results. The largest error was once again in IWBC with 8.50% and the least in UAB down with 1.93%.

The error observed in IWBC is likely a result of air leaking out of the wind tunnel. During the first experiments, it was discovered that air was transferring out of the wind tunnel by passing through the channels in the bus. Small stoppers were inserted into the channel to prevent air transfer. However, they may not have adequately sealed at higher air velocities.

As shown in Tables V and VI, changing convective heat loss calculation methods results in sizable error reduction. Error reduction ranged from 27.0% to 97.1% in forced convection and 11.3% to 81.0% in natural convection.

Authorized licensed use limited to: Georgia Institute of Technology. Downloaded on September 09,2020 at 14:47:32 UTC from IEEE Xplore. Restrictions apply.

TABLE VII
FORCED CONVECTION HEAT TRANSFER COEFFICIENTS CALCULATED WITH THE PROPOSED METHODOLOGY

Geometry	Size (in)	Temperature Rise over 40°C Ambient		
		30	50	70
Horizontal Rectangular				
	1/4 x 3	10.4337	10.3626	10.3016
	1/2 x 6	8.1296	8.0741	8.0267
	3/4 x 8	7.3297	7.2798	7.2370
Vertical Rectangular				
	1/4 x 3	13.7846	13.6977	13.6237
	1/2 x 6	10.6663	10.5990	10.5418
	3/4 x 8	9.5893	9.5288	9.4774
UAB Open				
	3 1/4 x 3 1/4 x 1/4	6.5084	6.3461	6.1992
	4 x 4 x 3/8	6.1918	6.1308	6.0770
	5 x 5 x 3/8	5.7909	5.7338	5.6835
UAB Closed				
	3 1/4 x 3 1/4 x 1/4	8.2841	8.1815	8.0337
	4 x 4 x 3/8	7.8650	7.7676	7.6807
	5 x 5 x 3/8	7.4383	7.3461	7.2639
IWBC				
	4 x 4 x 1/4	4.5014	4.4433	4.3915
	8 x 5 x 3/8	3.8115	3.7624	3.7185
	12 x 12 x 5/8	3.4581	3.4135	3.3737

TABLE VIII
NATURAL CONVECTION HEAT TRANSFER COEFFICIENTS CALCULATED WITH THE PROPOSED METHODOLOGY

Geometry	Size (in)	Temperature Rise over 40°C Ambient		
		30	50	70
Horizontal Rectangular				
	1/4 x 3	3.8370	4.1237	4.2969
	1/2 x 6	2.9079	3.1252	3.2565
	3/4 x 8	2.5918	2.7855	2.9025
Vertical Rectangular				
	1/4 x 3	5.7749	5.7749	6.5886
	1/2 x 6	4.9581	4.9581	5.6567
	3/4 x 8	4.6540	4.6540	5.3098
UAB Up				
	3 1/4 x 3 1/4 x 1/4	4.2116	4.8966	5.1226
	4 x 4 x 3/8	4.2760	4.6489	4.8634
	5 x 5 x 3/8	4.0440	4.3967	4.5996
UAB Down				
	3 1/4 x 3 1/4 x 1/4	3.7753	4.4017	4.6122
	4 x 4 x 3/8	3.8741	4.2315	4.4338
	5 x 5 x 3/8	3.7133	4.0558	4.2497
IWBC				
	4 x 4 x 1/4	2.3737	2.5689	2.6832
	8 x 5 x 3/8	1.9148	2.0722	2.1643
	12 x 12 x 5/8	1.6886	1.8274	1.9087

C. Method Comparison and Insights

The Nusselt correlations developed had improved accuracy over the flat plane method investigated. As demonstrated, changing bus orientation had a significant effect on error in ampacities calculated with flat plane correlations. By contrast, each Nusselt correlation was developed to a specific geometry and orientation. By discriminating between orientations, a study of the convective heat transfer coefficients can reveal insights previously unseen.

The convective heat transfer coefficient was calculated for each geometry using the developed Nusselt correlations. Bus size and temperature rise were varied. Forced convection calculations assumed a 2 ft/s air velocity and a 40 °C ambient air temperature. Table VII provides the results. Table VIII provides the same results for natural convection conditions.

The convective heat transfer coefficient decreases with increasing bus size and increasing temperature rise. Convective heat transfer $(Q_{convection})$ however increases as seen in (2).

Authorized licensed use limited to: Georgia Institute of Technology. Downloaded on September 09,2020 at 14:47:32 UTC from IEEE Xplore. Restrictions apply.

In forced convection, reorienting a rectangular bus from a horizontal orientation to a vertical position increases the heat transfer coefficient by 31.3% on average. Similarly, the convective heat transfer coefficient increases by 27.8% when UAB is placed in the closed position. Therefore, substation designers wishing to maximize bus ampacity should place rectangular bus in the vertical orientation and UAB in the closed orientation. However, unlike rectangular bus, UAB's orientation depends on wind direction, which is not always known or measured. Designers, engineers, and operators should select UAB open for conservative estimates in cases where wind direction is not known.

The same analysis was carried out under natural convection conditions. Once again, heat transfer is found to favor vertical orientation in rectangular bus with an average heat transfer coefficient increase of 68.9% over horizontal orientation. Heat transfer coefficients were found to be highest in UAB in the up position with an average percent increase of 9%.

VI. Conclusion

Prior to this study, no experimental work quantified the accuracy of the flat plane correlation method commonly employed to calculate substation bus ampacity. Through experiments, it was shown that the method often over predicts ampacity and varies with bus orientation. New Nusselt correlations were developed and shown to improve accuracy as well as account for bus orientation. While this work has improved the ampacity calculation method, advances can be made in other areas.

As bus orientation is shown to affect heat transfer, situations where the major bus axis is perpendicular to the ground as opposed to parallel need study in low air velocity environments at and close to natural convection conditions. At higher air velocity, this is less of a concern as buoyancy effects are dominated by the fluid's momentum. Other potential convection studies include a detailed study of heat transfer with wind direction, particularly when the flow is parallel to the major axis. The work in this study and previous work only considered the perpendicular flow direction.

The progress made by this study has the potential to improve Section 8 and Annexes B and C of IEEE std. 605.

References

[1] *IEEE Guide for Bus Design in Air Insulated Substations*, IEEE Standard 605, 2008.

[2] M. Prager, D. L. Pemberton, A. G. Craig, and N. A. Bleshman, "Thermal considerations for outdoor bus conductor design," *IEEE Trans. Power App. Syst.*, vol. 95, no. 4, pp. 1361–1368, Jul. 1976.

[3] M. Schmale, R. Puffer, and M. Heidemann, "Dynamic ampacity rating of conductor bars in highly loaded substations," in *Proc. 22nd Int. Conf. Exhib. Elect. Distrib.*, 2013, pp. 1–4.

[4] M. Muhammood, M. Kamarol, D. Ishak, and S. Masri, "Temperature rise prediction in 3-phase busbar system at 20 °C ambient temperature," in *Proc. IEEE Int. Conf. Power Energy*, 2012, pp. 736–740.

[5] I. C. Popa, A.-I. Dolan, D. Ghindeanu, and C. Boltaşu, "Thermal modeling and experimental validation of an encapsulated busbars system," in *Proc. 18th Int. Symp. Elect. App. Technol.*, 2014, pp. 1–4.

[6] A. Canova and L. Giaccone, "Numerical and analytical modeling of busbar systems," *IEEE Trans. Power Del.*, vol. 24, no. 3, pp. 1568–1578, Jul. 2009.

[7] *Facility Ratings*, North American Electric Reliability Corporation, NERC Standard FAC-008-3, 2017.

[8] M. E. Ali and H. Al-Ansary, "Experimental investigations on natural convection heat transfer around horizontal triangular ducts," *Heat Transfer Eng.*, vol. 31, no. 5, pp. 350–361, 2010.

[9] E. M. Sparrow, J. P. Abraham, and J. C. K. Tong, "Archival correlations for average heat transfer coefficients for non-circular and circular cylinders and for spheres in cross-flow," *Int. J. Heat Mass Transfer*, vol. 47, no. 24, pp. 5285–5296, 2004.

[10] G. R. Ahmed and M. M. Yovanovich, "Experimental study of forced convection from isothermal circular and square cylinders and toroids," *J. Heat Transfer*, vol. 119, pp. 70–79, 1997.

[11] F. Kreith and M. S. Bohn, *Principles of Heat Transfer*, 6th ed. Pacific Grove, CA, USA: Brooks/Cole, 2001.

Joseph Goldenburg (M'15) received the B.S. degree in mechanical engineering in 1992 and the M.S. in operations research in 1994, both from the Georgia Institute of Technology, Atlanta, Georgia. He is the Mechanical Section Leader with the Georgia Institute of Technology's National Electric Energy Testing Research and Applications Center. His employment experience includes Scientific Atlanta, Ciena, Siemens, and the Georgia Institute of Technology. He spent 19 years of his career in design, testing, and analysis of electrical and electronics products. His research interests include electrical systems cooling, thermal impact on structural mechanics, failure analysis, uncertainty quantification, and standards development.

Mr. Goldenburg is the immediate Past Chair of the ANSI C119.0 Committee on Connector Test Standards and is now the Vice-Chair of the ANSI C119 Executive Committee. He also serves on the ASTM B01 Committee for Overhead Conductors and the IEEE's Overhead Lines Committee. He is a licensed Professional Engineer with the State of Georgia. He has been a member of the IEEE Power and Energy Society since 2015 and attends the Overhead Lines Committee.

Tony Pribble (M'18) received the B.S. degree in mechanical engineering from Iowa State University, Ames, IA, USA, and he is currently working toward the M.S. degree in materials science and engineering (part time) at the Georgia Institute of Technology, Atlanta, GA, USA. He is a Mechanical Engineer with the National Electric Energy Testing Research and Applications Center, Georgia Institute of Technology. He is presently exploring areas of specialization within metals.

Authorized licensed use limited to: Georgia Institute of Technology. Downloaded on September 09,2020 at 14:47:32 UTC from IEEE Xplore. Restrictions apply.